JOURNAL OF Materials CHEMISTRY

Novel red-emitting fluorene-based copolymers

Qiong Hou, Yishe Xu, Wei Yang, Min Yuan, Junbiao Peng and Yong Cao*

Institute of Polymer Optoelectrionic Materials and Devices, South China University of Technology, Guangzhou, China 510640. E-mail: poycao@scut.edu.cn

Received 22nd April 2002, Accepted 3rd July 2002
First published as an Advance Article on the web 13th August 2002

A series of novel soluble conjugated copolymers derived from 9,9-dioctylfluorene (DOF) and 4,7-di-2-thienyl-2,1,3-benzothiadiazole (DBT) were synthesized by a palladium-catalyzed Suzuki coupling reaction with different feed ratios of DOF to DBT. Owing to exciton confinement on the DBT site, exciton emission is centred on the DBT chromophore and gives rise to saturated red emission. Polyfluorene fluorescence is quenched completely at DBT concentrations as low as 1% in the solid film. Devices based on these copolymers emit a saturated red light. Chromaticity coordinates are around $x = 0.70$, $y = 0.30$ for the copolymers. The emission peaks are shifted from 628 nm to 674 nm when DBT content increases from 1 to 35%. The highest quantum efficiency achieved with device configuration of ITO/PEDT/PFO-DBT/Ba/Al was 1.4% for the copolymer with 15% DBT content.

Introduction

In recent years, electroluminecent polymers have attracted great attention due to their possible utilization in flat panel displays. Polyfluorenes are promising new materials for light-emitting diodes because of their thermal and chemical stability and exceptionally high fluorenscence quantum yields (0.6–0.8) in thin solid films.[1] Normally, polyfluorene homopolymers have large bandgaps and emit blue light. The emission color of polyfluorenes can be tuned over the entire visible region by incorporating narrow band-gap comonomers into the polyfluorene backbone.[2,3] The most widely used narrow band-gap comonomers are a variety of aromatic heterocycles such as thiophene,[4–17] ethylenedioxythiophene[4–9] and benzothiadiazole.[15–19] In most of these reports the copolymers were alternating A–B-type copolymers which show low electroluminescence (EL) efficiencies. For example copolymerization of fluorene with 4,7-di-2-thienyl-2,1,3-benzothiadiazole has been reported in the patent literature by the Dow Chemical group.[19] The three-component copolymer (fluorene–benzothiadiazole–dithienylbenzothiadiazole) was prepared and white light-emitting devices were fabricated from the polymer blend of such a copolymer with a blue emitter. The power efficiences for devices from such a blend increased to 0.2–0.3 Lm W^{-1}.[19] Recently, we reported the synthesis and properties of copolymers with carbazole as a main chain building unit and DBT as a narrow band-gap component.[20]

In this paper we report the synthesis and characterization of copolymers derived from fluorene and 4,7-di-2-thienyl-2,1,3-benzothiadiazole (DBT, structure in Scheme 1) in less than 50% in the polymer composition by the Suzuki coupling reaction. A special feature of the Suzuki coupling is that it allows an alternating type of copolymer to be obtained in the case of A–B comonomers, while typical cross-coupling of dibromides provides a multiblock copolymer. In the case of Suzuki coupling, each individual narrow band-gap unit is separated on both sides by wide band-gap segments, once the narrow band-gap component is less or equal to 50% in the copolymer. In this case we could expect that the narrow band-gap unit functions as an exciton trap which allows efficient intramolecular energy transfer from the fluorene segment to the DBT unit. Devices based on the copolymers emit a saturated red light. The highest quantum efficiency achieved in the device of configuration ITO/PEDT/PFO-DBT/Ba/Al (ITO: indium tin oxide; PEDT: poly(3,4-ethylenedioxythiophene)–polystyrene sulfonate) was 1.4% for a copolymer with 15% DBT content.

Experimental

Instrumentation

^{1}H and ^{13}C NMR spectra were recorded on a Varian Inova 500 or Bruker DRX 400 spectrometer in deuterated chloroform solution at 298 K. Number-average ($\bar{M}_n$) and weight-average ($\bar{M}_w$) molecular weights were determined by Waters GPC 2410 in THF using a calibration curve of polystyrene standards. Elemental analysis was performed on a Vario EL Elemental Analysis Instrument (ELEMENTAR Co.) or on an Antek 7000S/N (ANTEK Co.). UV-visible absorption spectra were recorded on a HP 8453 spectrophotometer. Cyclic voltammetry was performed using a CHI660A electrochemical workstation with platinum electrodes at a scan rate of 50 mV s^{-1} against a calomel reference electrode with an anhydrous and nitrogen-saturated solution of 0.1 M tetrabutylammonium hexafluorophosphate (Bu_4NPF_6)–acetonitrile (CH_3CN). The deposition of polymers on the electrode was done by the evaporation of a dilute chloroform solution. The PL quantum yields were determined using an Integrating sphere IS080 (Labsphere) with 325 nm excitation from a HeCd laser (Mells Griod). EL efficiency and brightness measurements were carried out with a calibrated silicon photodiode. Photoluminescence (PL) and EL spectra were recorded on an Instaspec IV CCD spectrophotometer (Oriel Co.).

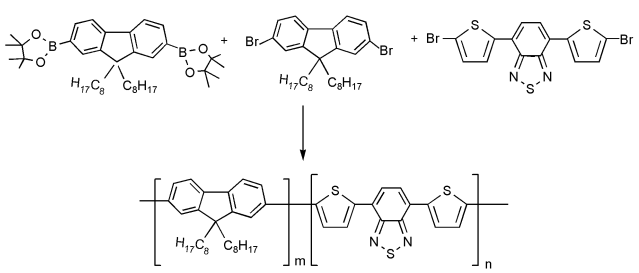

Comonomer ratio: 99/1(PFO-DBT1), 95/5(PFO-DBT5), 90/10(PFO-DBT10), 85/15(PFO-DBT15), 75/25(PFO-DBT25), 65/35(PFO-DBT35)

Scheme 1 Synthetic route of copolymers.

DOI: 10.1039/b203862e

Materials

Fluorene, Bu^nLi, *n*-octylbromide, iron powder and 2-isopropoxy-4,4,5,5-tetramethyl-1,3,2-dioxaborolane were purchased from Aldrich Co. Tetrakis(triphenylphosphine)palladium was obtained from TCI Co. Thiophene, tributylchlorostannane, 2,1,3-benzothiadiazole, $PdCl_2(PPh_3)_2$ and Aliquat 336 were purchased from Acros Co. *N*-Bromosuccinimide and bromine were used as received. Anhydrous tetrahydrofuran was distilled over sodium–benzophenone under nitrogen prior to use. Chloroform, carbon tetrachloride and toluene were distilled over calcium chloride. 9,9-Dioctylfluorene[21] (**1**), 2,7-dibromo-9,9-dioctylfluorene[21] (**2**), tributyl(2-thienyl)stannane[22] (**3**) and 4,7-dibromo-2,1,3-benzothiadiazole[23] (**4**) were prepared following the already published procedures.

2,7-Bis(4,4,5,5-tetramethyl-1,3,2-dioxaborolan-2-yl)-9,9-dioctylfluorene (5)[21]

To a solution of 2,7-dibromo-9,9-dioctylfluorene (**2**, 5.6 g, 10.22 mmol) in THF (130 mL) at −78 °C, Bu^nLi (19.7 mL of a 1.6 M solution in hexane, 31.45 mmol) was added dropwise. The mixture was stirred at −78 °C for 2 h. 2-Isopropoxy-4,4,5,5-tetramethyl-1,3,2-dioxaborolane (25 ml, 123.24 mmol) was added rapidly to the solution. The mixture was stirred at −78 °C for 2 h, then it was warmed to room temperature and stirred for 36 h. The mixture was poured into water and it was extracted with ether. The organic layer was washed with brine and dried over anhydrous magnesium sulfate. The solvent was removed under reduced pressure, and the residue was recrystallized from tetrahydrofuran and methanol, then it was purified by column chromatography (silical gel, 10% ethyl acetate in hexane) to give the title product as a white solid in 46% yield. Mp 128–131 °C. ^{1}H NMR $\delta(CDCl_3)$: 7.80 (d, 2H), 7.74 (s, 2H), 7.71 (d, 2H), 1.99 (m, 4H), 1.39 (s, 24H), 1.22–1.00 (m, 20H), 0.81 (t, 6H), 0.56 (m, 4H). ^{13}C NMR $\delta(CDCl_3)$: 150.86, 144.30, 134.04, 129.29, 119.77, 84.11, 55.57, 40.49, 32.18, 30.33, 29.58, 25.33, 23.98, 22.99, 14.48. Element Anal. Calcd for $C_{41}H_{64}O_4B_2$: C, 76.74%; H, 10.04%. Found: C, 76.44%; H, 9.90%.

4,7-Di-2-thienyl-2,1,3-benzothiadiazole (6)[24]

To a solution of 4,7-dibromo-2,1,3-benzothiadiazole (2 g, 6.8 mmol) and tributyl(2-thienyl)stannane (6.1 g, 16.4 mmol) in THF (50 ml), $PdCl_2(PPh_3)_2$ (97 mg, 2 mol%) was added. The mixture was refluxed under a nitrogen atmosphere for 3 h. After removal of the solvent under reduced pressure, the residue was purified by column chromatography on silica gel (eluent CH_2Cl_2–hexane, 1 : 1). Recrystallization from ethanol gave the title compound (1.8 g, 88%) as red needles. Mp 124–125 °C. ^{1}H NMR $\delta(CDCl_3)$: 8.11 (dd, 2H), 7.87 (s, 2H), 7.46 (dd, 2H), 7.21 (dd, 2H). ^{13}C NMR $\delta(CDCl_3)$: 126.15, 126.38, 127.21, 127.90, 128.42, 139.75, 153.02. Element Anal. Calcd for $C_{14}H_8N_2S_3$: C, 55.97%; H, 2.68%; N, 9.32%; S, 32.02%. Found: C, 56.34%; H, 2.82%; N, 9.50%; S, 32.38%.

4,7-Bis(5-bromo-2-thienyl)-2,1,3-benzothiadiazole (7)[19]

To a mixture of chloroform (52 ml) and acetic acid (52 ml), 4,7-di-2-thienyl-2,1,3-benzothiadiazole (2 g, 6.67 mmol) was added under a nitrogen flow. After the solid dissolved completely, *N*-bromosuccinimide (NBS, 2.5 g, 14.01 mmol) was added in one portion. The reaction mixture was stirred at room temperature overnight, and the dark red precipitate formed was filtered off and recrystallized from DMF to give the title compound (1 g, 33%) as shiny red crystals. Mp 251–252 °C. ^{1}H NMR (500 MHz) $\delta(CDCl_3)$: 7.81 (dd, 2H), 7.78 (s, 2H), 7.15 (dd, 2H). Element Anal. Calcd for $C_{14}H_6N_2S_3Br_2$: C, 36.70%; H, 1.32%; N, 6.11%; S, 20.99%; Br, 34.88%. Found: C, 36.94%; H, 1.63%; N, 6.21%; S, 21.70%; Br, 33.52%.

Polymer synthesis[21]

Carefully purified 2,7-dibromo-9,9-dioctylfluorene (**2**), 2,7-bis(4,4,5,5-tetramethyl-1,3,2-dioxaborolan-2-yl)-9,9-dioctylfluorene (**5**), 4,7-bis(5-bromo-2-thienyl)-2,1,3-benzothiadiazole (**7**) and $(PPh_3)_4Pd(0)$ (0.5–1.5 mol%) ,and Aliquat 336 were dissolved in a mixture of toluene and an aqueous solution of 2 M Na_2CO_3. The mixture was first put under an argon atmosphere and refluxed with vigorous stirring for 72 h. Then 2,7-bis(4,4,5,5-tetramethyl-1,3,2-dioxaborolan-2-yl)-9,9-dioctylfluorene and bromobenzene were added to end-cap the polymer chain. The whole mixture was poured into methanol. The precipitated material was recovered by filtration through a funnel and washed with acetone to remove oligomers and catalyst residues (yield: 70–83%). The resulting polymers were soluble in conventional organic solvents (toluene, chloroform, and tetrahydrofuran). The results of the elemental analyses for sulfur (or nitrogen) and carbon for each copolymer were used for calculating the actual copolymer composition. Element Anal. Found: for PFO-DBT1: C, 86.36%; H, 9.78%; N, 0.12%; S, 0.27% ; for PFO-DBT5: C, 86.99%; H, 9.93%; N, 0.51%; S, 1.18% (by Vario EL), 1.23% (by Antek 7000S/N); for PFO-DBT10: C, 85.60%; H, 9.90%; N, 0.50%, S, 1.81%; for PFO-DBT15: C, 83.90%; H, 9.22%; N, 1.04%; S, 3.90%; for PFO-DBT25: C, 81.14%; H, 8.38%; N, 1.85%; S, 6.49%; for PFO-DBT35: C, 75.57%; H, 7.76%; N, 2.72%; S, 9.07%.

Results and discussion

Synthesis and characterization of copolymers

High molecular weight, readily soluble copolymers ($\bar{M}_n$ = 11000–35000) of different compositions were prepared from 2,7-dibromo-9,9-dioctylfluorene (DOF), 2,7-bis(4,4,5,5-tetramethyl-1,3,2-dioxaborolan-2-yl)-9,9-dioctylfluorene and narrow band gap comonomer 4,7-bis(5-bromo-2-thienyl)-2,1,3-benzothiadiazole (DBT) using palladium catalyzed Suzuki coupling methods (Scheme 1). The comonomer feed ratios of DOF to DBT are 99 : 1, 95 : 5, 90 : 10, 85 : 15, 75 : 25 and 65 : 35 respectively, and the corresponding copolymers were named PFO-DBT1, PFO-DBT5, PFO-DBT10, PFO-DBT15, PFO-DBT25 and PFO-DBT35 respectively. For these copolymers, *n*-octyl substituents in the 9-position of fluorene were employed to improve the solubility of the resulting copolymers. At the end of the polymerization, 2,7-bis(4,4,5,5-tetramethyl-1,3,2-dioxaborolan-2-yl)-9,9-dioctylfluorene was added to remove bromine end groups and bromobenzene was added as a monofunctional end-capping reagent to remove boronic ester end groups, because boron and bromine units could quench emission and contribute to excimer formation in LED applications.[25] The starting monomer ratios have been adjusted in order to investigate the effect of copolymer composition on the physical and optical properties. The actual ratio of DOF : DBT in the copolymer, calculated from elemental analysis, is very close to the feed ratio, as listed in Table 1. The incorporation of DBT into the polyfluorene main chain was also monitored by UV spectroscopy

Table 1 Molecular weights of the copolymers

Copolymer	$\bar{M}_n$ ($\times 10^3$)	$\bar{M}_w/\bar{M}_n$	DOF : DBT in the feed composition	DOF : DBT in the copolymers[a]
PFO-DBT1	23	2.6	99 : 1	98.9 : 1.1
PFO-DBT5	35	3.1	95 : 5	95.2 : 4.8
PFO-DBT10	33	2.7	90 : 10	92.6 : 7.4
PFO-DBT15	34	2.6	85 : 15	85.7 : 14.3
PFO-DBT25	29	2.4	75 : 25	75.3 : 24.7
PFO-DBT35	11	1.7	65 : 35	64.5 : 35.5

[a]Calculated from results of elemental analysis.

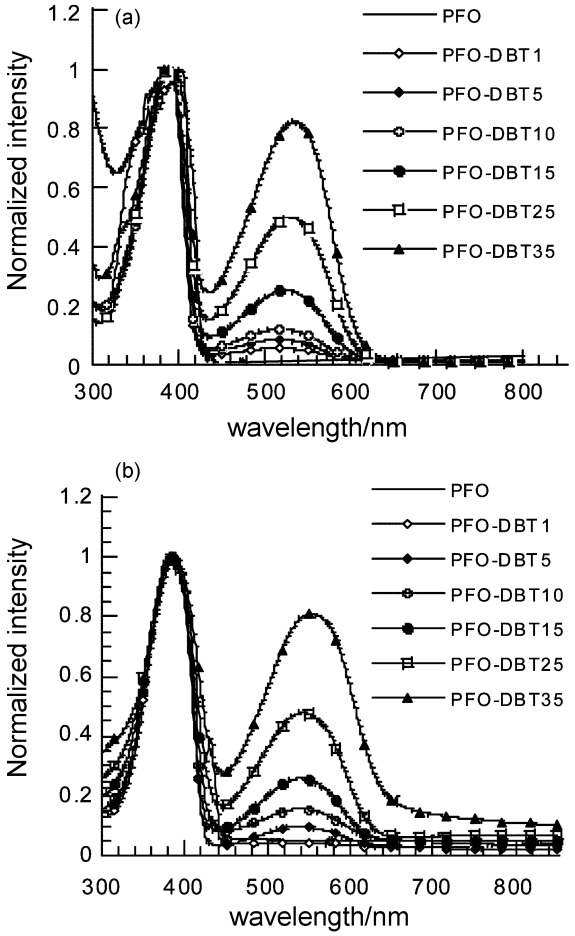

Fig. 1 (a) UV-Vis absorption spectra for the copolymers in $CHCl_3$ solution. (b) UV-Vis absorption spectra for the copolymers in solid state films.

(λ_{max}(oligofluorene segments) = 380 nm, λ_{max} (incorporated DBT) = 540 nm) (Fig. 1). Most of the polymers exhibit a relatively high molecular weight with a polydispersity index ($\bar{M}_w/\bar{M}_n$) from 1.7 to 3.1 (Table 1). These polydispersity indexes are consistent with a polycondensation reaction.

Optical and photoluminescent properties

The UV-Visible absorption properties are summarized in Table 2 and Fig. 1. All the copolymers show similar absorption spectra in solution (Fig. 1a) and in the solid films (Fig. 1b). The absorption spectra of the copolymers measured in thin films display two absorption peaks. The absorption peaks at *ca.* 380 nm are attributed to the fluorene segment, and the additional long wavelength absorption bands at *ca.* 540 nm are attributed to the DBT unit incorporated into the polyfluorene main chain. Moreover, the absorption intensity at 540 nm increased gradually with increasing concentration of DBT in the polymer backbone. In the case of the copolymer containing one percent of DBT in the copolymer main chain, the presence of the DBT unit is not apparent from the absorption spectrum in the solid film (Fig. 1b), however, a weak 540 nm peak is clearly seen in the solution spectrum of 1% DBT copolymer (Fig. 1a). The two distinguishable absorption features of the copolymers demonstrate that the electronic configurations of the two components, DOF and DBT, in the copolymers are not mixed.

The photoluminescent (PL) spectra of the polymers in thin films and in $CHCl_3$ solution, produced by excitation with the 325 nm line of the HeCd laser, are presented in Fig. 2a and 2b respectively. In thin solid films, polyfluorene emission was completely quenched and PL emission consists exclusively of DBT emission at DBT concentrations as low as 1% (Fig. 2a). In $CHCl_3$ solution with a copolymer concentration of 1×10^{-5} mol L^{-1}, PL emission consists of both fluorene and DBT emission in the PFO-DBT1 and PFO-DBT5 copolymers (Fig. 2b). For copolymers with DBT content equal to or greater than 10%, PL emission consists exclusively of DBT emission at a concentration of 1×10^{-5} mol L^{-1} (Fig. 2b). Since, for the PFO-DBT1 copolymer with a number average molecular weight of 2.3×10^4 (Table 1), statistically only one third of the polymer chain contains the copolymer with the DBT unit, the interchain interaction must play some role in PL quenching. In Fig. 3, the PL spectra of PFO-DBT1 (Fig. 3a) and PFO-DBT25 (Fig. 3b) are compared at different concentrations. Polyfluorene emission was completely quenched when the

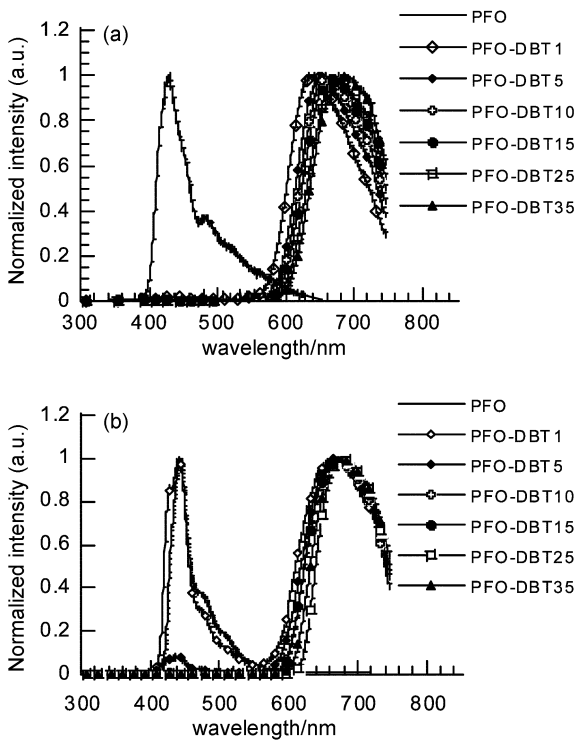

Fig. 2 (a) PL spectra of the copolymers in solid state films. (b) PL spectra of the copolymers in $CHCl_3$ solution at a concentration of 1×10^{-5} mol L^{-1}.

Table 2 UV-Vis and electrochemical properties of the copolymers

Copolymer	λ_{absmax}/nm	Optical band gap[a]/eV	E_{ox}/V	E_{HOMO}/eV	E_{LUMO}[b]/eV
PFO-DBT1	382, —	2.93, —	1.32, —	−5.72, —	−2.79, —
PFO-DBT5	382, 535	2.93, 2.08	1.28, —	−5.65, —	−2.72, —
PFO-DBT10	384, 536	2.93, 2.07	1.32, 1.21	−5.72, −5.61	−2.79, −3.54
PFO-DBT15	382, 538	2.91, 2.03	1.31, 1.15	−5.71, −5.55	−2.80, −3.52
PFO-DBT25	384, 542	2.88, 2.02	1.32, 1.10	−5.72, −5.50	−2.84, −3.48
PFO-DBT35	388, 551	2.88, 2.01	1.30, 1.07	−5.70, −5.47	−2.82, −3.46

[a]Estimated from the onset wavelength of optical absorption in the solid state film. [b]Calculated from the HOMO level and optical band gap.

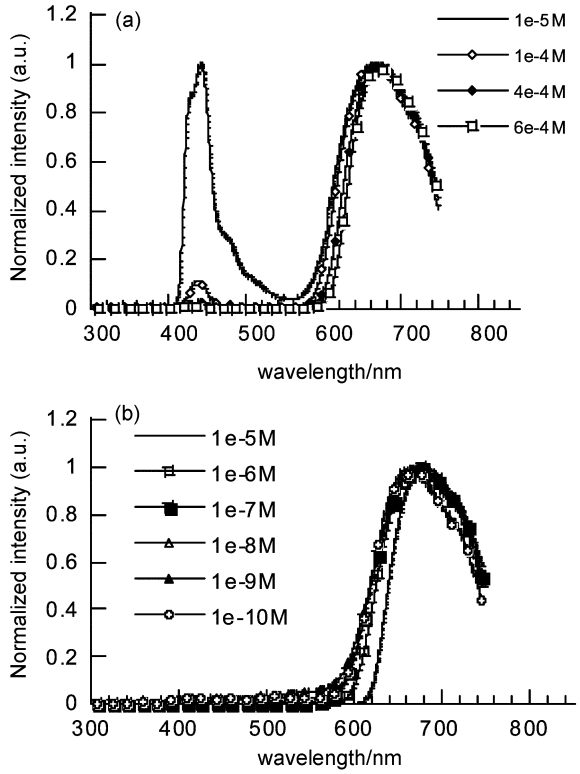

Fig. 3 (a) PL spectra of polymer PFO-DBT1 in $CHCl_3$ solution of different concentrations. (b) PL spectra of polymer PFO-DBT25 in $CHCl_3$ solution at different concentrations.

Table 3 Concentration of copolymers at which PFO fluorescence is completely quenched

Copolymer	Concentration of copolymer at which PFO fluorescence is completely quenched/mol L^{-1}
PFO-DBT1	4×10^{-4}
PFO-DBT5	5×10^{-5}
PFO-DBT10	5×10^{-6}
PFO-DBT15	1×10^{-7}
PFO-DBT25	1×10^{-10}

concentration of PFO-DBT1 is equal to or greater than 4×10^{-4} mol L^{-1} (Fig. 3a). In case of PFO-DBT25 the PFO fluorescence was practically absent at concentrations as low as 1×10^{-10} mol L^{-1} (Fig. 3b). Table 3 lists the critical concentration at which polyfluorene fluorescence was completely quenched. The observed concentrations are much lower than the "overlap threshold concentration" of typical non-conjugated polymers.[26] Detailed analysis of solution properties and energy transfer in solution are in progress and will be presented elsewhere. These facts seem to suggest that intramolecular energy transfer plays a major role in such copolymers prepared by the cross-coupling method (Suzuki coupling). The DBT unit serves as a powerful trap. Excitons are confined in the vicinity of the DBT unit isolated on both sides by the fluorene segment and give rise to red light emission. Significant enhancement of the external quantum efficiencies of electroluminescence by exciton confinement in the random copolymers that have different energy gap region within a single chain was first reported by Burn *et al.*[27]

Table 4 lists the PL efficiencies obtained with 325 nm excitation using the HeCd laser. The PL efficiencies decrease quickly with increasing DBT content in the copolymers from 11% for PFO-DBT1 to 4% for PFO-DBT35.

Electrochemical properties

The electrochemical behavior of the copolymers was investigated by cyclic voltammetry (CV). Except for the copolymers with 1 and 5% DBT, all of the copolymers show two p-doping processes. Table 2 summarizes the oxidation potentials derived from the onset in the cyclic voltammograms of the copolymers. For copolymers with DBT content equal to or greater than 10%, the first onset of the p-doping processes decreases with increasing DBT content from 1.21 V for PFO-DBT10 to 1.07 V for PFO-DBT35. The second onset of the oxidation process is almost constant for all of the copolymers at about 1.30–1.32 V. For PFO-DBT1 only one peak can be observed in the voltammogram. The position of the onset of this peak is the same (1.31 V) as the second onset with high DBT content. This peak is attributed to p-doping of the DOF segments. It is slightly unusual for PFO-DBT5, for which only one oxidation peak is observed, the onset of which is moved to 1.28 V. This peak is a result of the mixing of both oxidation processes in the voltammogram. We were unable to record n-doping processes after many attempts. The energies of the HOMO levels, calculated according to an empirical formula ($E_{HOMO} = -e(E_{ox} + 4.4)$ (eV)),[28] are listed in Table 2. In order to get some idea about LUMO energies in these copolymers, they were estimated from the optical band gap and HOMO energies. The results are also listed in Table 2. The HOMO energies, 5.7 eV, calculated from the second onset in the voltammograms are very similar to the data reported for polyfluorene homopolymers, $E_{ox} = 1.4$ V, $I_p = 5.8$ eV.[29] HOMO levels corresponding to the DBT unit are slightly decreasing with increasing DBT content *e.g.* $E_{HOMO} = 5.47$ eV for PFO-DBT35. The energies of the LUMO levels corresponding to the DOF segments remain almost unchanged for the copolymers with different DBT contents, while the LUMO levels due to the DBT unit decrease with increasing DBT content. Bearing in mind that a single DBT unit is isolated on both sides by fluorene segments, the change in HOMO and LUMO levels for the DBT units must originate from interchain interactions. Two well-defined oxidation processes in the cyclic voltammograms and the similarity of the E_{HOM-} values for the DOF segment in the copolymers and for DOF in the homopolymer demonstrate again that the electronic configuration of the two components, DOF and DBT, in the copolymers are not mixed. This is very consistent with the two distinct absorption peaks in the UV-Vis spectra (Fig. 1).

Table 4 Optical Properties of the copolymers

	Photoluminescence		Electroluminescence		Chromaticity coordinate	
Copolymer	λ_{Plsmax}/nm	Q_{PLsmax}(%)	λ_{Elsmax}/nm	Q_{extmax}(%)	x	y
PFO-DBT1	635	11.4	628	0.5	0.67	0.32
PFO-DBT5	651	12.5	643	0.6	0.70	0.31
PFO-DBT10	655	8.6	652	0.9	0.70	0.30
PFO-DBT15	678	7.9	663	1.4	0.70	0.29
PFO-DBT25	678	5.2	669	0.6	0.70	0.29
PFO-DBT35	685	4	674	0.5	0.70	0.29

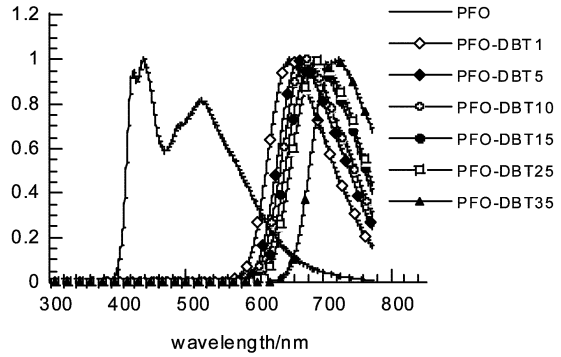

Fig. 4 EL spectra of devices from the copolymers.

Electroluminescent properties

A single layer device was fabricated in the configuration ITO/PEDT/PFO-DBT/Ba/Al. The EL spectra from such device are presented in Fig. 4. A saturated red emission was obtained for all of the copolymers. EL peaks are 10 nm blue shifted in comparison with PL peaks with slightly larger bandwidth (*cf.* Fig 2 and 4). Emission peaks shift from 628 nm for PFO-DBT1 to 674 nm for PFO-DBT35 (Fig. 4 and Table 4). The chromaticity coordinates changed from $x = 0.67, y = 0.32$ for PFO-DBT1 to $x = 0.70, y = 0.29$ for PFO-DBT35. Table 4 lists the emission maximum and chromaticity coordinates for each copolymer. It is very important to note the fact that EL emission is exclusively from the DBT unit and PFO emission is completely quenched. The PFO emission is completely quenched even at 1% DBT loading. This is very similar to what was observed for the PL spectra. McGehee[30] and O'Brien[31] and their co-workers reported large differences between the PL and EL spectra at low doping concentrations for Eu-complex/CNPPP and PtOEP/PFO devices. For these systems host PL emissions were quenched completely only at much higher doping concentrations than those of EL spectra. This is quite common for dye-doped polymer systems.[30,31] The differences in the PL and EL spectra at low doping concentrations were attributed to the differences in the recombination zone for photo- and electric excitations.[30] For copolymers in this study, as mentioned above, energy transfer probably occurs mainly within the polymer chain *via* intramolecular energy transfer. Again this fact demonstrates that intramolecular energy transfer in the PFO-DBT copolymer is a very quick and efficient process. As a result the generated excitons are efficiently confined to DBT sites.

We note also that both PL (in solution and in solid films) and EL emission are red-shifted with increasing DBT content in polymer chains (Fig. 2 and 4). This fact is consistent with the small change in HOMO (decreasing) and LUMO (increasing) levels with increasing DBT content (Table 2). We note also a slight red shift of the PL peaks with increasing copolymer concentration (Fig. 3a and Fig. 3b). This fact indicates that the red shift of the PL spectra must be related to the interchain interactions too.

Preliminary device data are promising for application. The external EL efficiencies in the device of configuration ITO/PEDT/PFO-DBT/Ba/Al vary with copolymer composition. The device performance is compared in Table 5 at current density of 33.3 mA cm^{-2} (5 mA for a device with an active area of 0.15 cm^2) .The external quantum efficiencies increase initially with DBT content, then gradually decrease. The highest external EL quantum efficiency was 1.4% and the luminance of 256 cd m^{-2} at a bias of 5.1V for the device containing copolymer with 15% DBT content (Table 5). The highest luminance can reach 3780 cd m^{-2} at 8.2 V. The device containing copolymer with 1% DBT content gave only an external QE of 0.5%, despite it having the highest PL efficiency from this series. The existence of a maximum in the curve of QE *vs.* DBT content indicates that there are two opposite processes controlling the device efficiency. Since the HOMO level decreases with increasing DBT contents, the barrier height for hole injection decreases accordingly. As the LUMO level does not change very much with increasing DBT content (Table 2), the electron injection should not change for copolymers with different DBT contents. However, we note that PL efficiencies decrease remarkably with increasing DBT content. Thus, PL quenching leads to a decrease in EL efficiency with increasing DBT content. The increase in the operating voltage with increasing DBT content seems to support such an interpretation.

Table 5 Device performance of PFO-DBT copolymers

	Device performance[a]			
Copolymer	Bias/V	*I*/mA cm^{-2}	Luminance/cd m^{-2}	QE_{ext} (%)
PFO-DBT1	6.1	33.3	91	0.5
PFO-DBT5	7.2	33.3	130	0.6
PFO-DBT10	7.7	33.3	167	0.9
PFO-DBT15	5.1	33.3	259	1.4
PFO-DBT25	3.1	33.3	109	0.6
PFO-DBT35	3.3	33.3	103	0.5

[a]Device structure: ITO/PEDT/PFO-DBT/Ba/Al, active area 0.15 cm^2.

Conclusions

The synthesis of high molecular weight, readily soluble copolymers of 9,9-dioctylfluorene and the low band gap comonomer DBT can be accomplished by Pd-catalyzed Suzuki coupling reactions. The efficient energy transfer due to exciton trapping on narrow band-gap DBT sites has been observed. Polyfluorene fluorescence is quenched completely at DBT concentrations as low as 1% in the solid state film. All of the copolymers emit saturated red color. Preliminary device characteristics are promising for utilization. Devices fabricated with copolymer with 15% DBT content shows the highest external quantum efficiency at 1.4%. Further improvement by manipulating the polymer/electrode interface is in progress.

Acknowledgements

This research was supported by the Natural Science Foundation of China (Project No. 29992530-6) and Guangdong Province (Project No. 990623).

References

1 G. Klärner, J.-I. Lee, M. H. Davey and R. D. Miller, *Adv. Mater.*, 1999, **11**, 115–119.
2 G. Klaerner and R. D. Miller, *Macromolecules*, 1998, **31**, 2007–2009.
3 M. T. Bernius, M. Inbasekaran, J. O. Brien and W. Wu, *Adv. Mater.*, 2000, **13**, 1737.
4 F. Larmat, J. R. Reynolds, B. A. Reinhardt, L. L. Brott and S. J. Clarson, *J. Polym. Sci., Part A: Polym. Chem.*, 1997, **35**, 3627–3636.
5 B. Tsuie, J. L. Reddinger, G. A. Stozing, J. Soloducho, A. R. Katritzky and J. R. Reynolds, *J. Mater. Chem.*, 1999, **9**, 2189–2200.
6 A. Donat-Bouillud, I. Lévesque, Y. Tao and M. D'Iorio, *Chem. Mater.*, 2000, **12**, 1931–1936.
7 P. Blondin, J. Bouchard, S. Beaupré, M. Belletête, G. Durocher and M. Leclerc, *Macromolecules*, 2000, **33**, 5874–5879.
8 I. Lévesque, A. Donat-Bouillud, Y. Tao, M. D'Iorio, S. Beaupré, P. Blondin, M. Ranger, J. Bouchard and M. Leclerc, *Synth. Met.*, 2001, **122**, 79–81.
9 M. Leclerc, *J. Polym. Sci., Part A: Polym. Chem.*, 2001, **39**, 2867–2873.
10 M. Ranger and M. Leclerc, *Can. J. Chem.*, 1998, **76**, 1571–1577.

11 B. Liu, W.-L. Yu, Y.-H. Lai and W. Huang, *Macromolecules*, 2000, **33**, 8945–8952.
12 B. Liu, W.-L. Yu, J. Pei, Y.-H. Lai, W. Huang, Y.-H. Niu and Y. Cao, *Mater. Sci. Eng., B*, 2001, **85**, 232–235.
13 A. Charas, N. Barbagallo, J. Morgado and L. Alcácer, *Synth. Met.*, 2001, **122**, 23–25.
14 X. W. Zhan, Y. Q. Liu, D. B. Zhu, X. Z. Jiang and A. K.-Y. Jen, *Synth. Met.*, 2001, **124**, 323–327.
15 M. Bernius, M. Inbasekaran, E. Woo, W. S. Wu and L. Wujkowski, *J. Mater. Sci.: Mater. Electron.*, 2000, **11**, 111–116.
16 M. Inbasekaran, W. S. Wu and E. P. Woo, *US Pat.*, 1998, 5777070.
17 K. S. Whitehead, M. Grell, D. D. C. Bradley, M. Inbasekaran and E. P. Woo, *Synth. Met.*, 2000, **111–112**, 181–185.
18 I. S. Millard, *Synth. Met.*, 2000, **111–112**, 119–123.
19 M. Inbasekaran, E. P. Woo, W. S. Wu and M. T. Bernius, PCT application, 2000, W0046321A1.
20 J. Huang, Y. Xu, Q. Hou, W. Yang and Y. Cao, *Macromol. Rapid Commun.*, in the press.
21 M. Ranger, D. Rondeau and M. Leclerc, *Macromolecules*, 1997, **30**, 7686–7691.
22 J. T. Pinhey and E. G. Roche, *J. Chem. Soc., Perkin, Trans. 1*, 1988, 2415–2421.
23 K. Pilgram, M. Zupan and R. Skile, *J. Heterocycl. Chem.*, 1970, **6**, 629.
24 C. Kitamura, S. Tanaka and Y. Yamashita, *Chem. Mater.*, 1996, **8**, 570–578.
25 W. Yang, *Book of Abstracts, International Conference on Science and Technology of Synthetic Metals (ICSM2002)*, Fudan University Press, Shanghai, China, 2002, p. 21.
26 Pierre-Gilles de Gennes, *Scaling Concepts in Polymer Physics*, Cornell University Press, Ithaca, NY, 1979, pp. 76–80.
27 P. L. Burn, A. B. Holmes, A. Kraft, D. D. C. Bradley, A. R. Brown, R. H. Friend and R. W. Gymer, *Nature*, 1992, **356**, 47.
28 D. M. Leeuw, M. M. J. Simenon, A. R. Brown and R. E. F. Einerhand, *Synth. Met.*, 1997, **87**, 53.
29 S. Janietz, D. D. C. Bradley, M. Grell, C. Giebeler, M. Inbasekaran and E. P. Woo, *Appl. Phys. Lett.*, 1998, **73**, 2453.
30 M. D. McGehee, T. T. Bergstedt, C. Zhang, A. P. Saab, M. B. O'Regan, G. C. Bazan, V. I. Srdanov and A. J. Heeger, *Adv. Mater.*, 1999, **11**, 1349.
31 D. F. O'Brien, C. Giebeler, R. B. Fletcher, A. J. Cadby, L. C. Palilis, D. G. Lidzey, P. A. Lane, D. D. C. Bradley and W. Blau, *Synth. Met.*, 2001, **116**, 379–383.